

CHAPTER-2

Theoretical Details

This chapter discusses various theories related to conduction mechanism and various formalisms of impedance spectroscopy.

INTRODUCTION

Understanding electrical conduction mechanism in polymer electrolytes is an imposing challenge. Ionic conductivity is the key facet which must be probed inventively to understand mechanism of conduction in polymer electrolytes. Ion transport mechanism offers wide and inquisitive insights in to this complicated process occurring in liquid solutions, molten salts or crystalline solid electrolytes.

2.1 Ionic Conductivity

Ability of a material to conduct electric current is defined as its conductivity. Ion transport process occurring in an electrolyte is due to the random migration of ions activated by thermal energy. Ionic conductivity is the ion transport occurring under some electric field. In solid materials, ions occupy fixed positions in the lattice and are in-capable of movement. Ion conduction occurs if the ions can escape from their current sites and hop on to the adjacent available site. Two mechanisms vacancy and interstitial (*Cahn and Haasen, 1996*) can explain this movement of ions through the lattice. The mechanisms are schematically represented in Fig. 2.1.

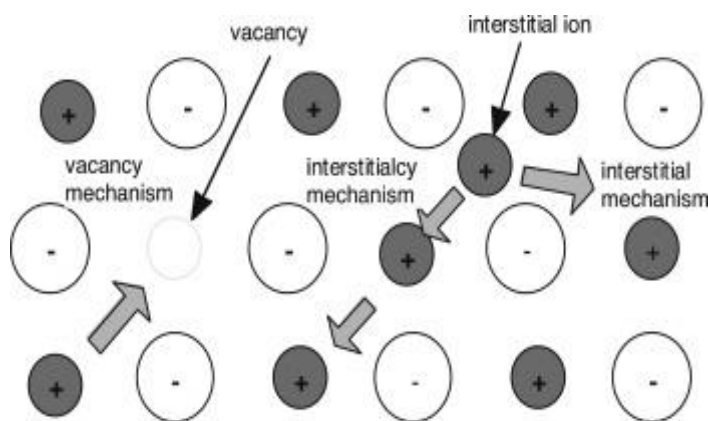


Fig. 2.1 Vacancy and Interstitial mechanism for ion motion.

<https://www.sciencedirect.com/topics/chemistry/ionic-crystal>

The following basic conditions are necessary for ion conduction:

1. Large number mobile ions of one species.
2. Large number of available empty sites.
3. The empty and occupied sites must be equi-energy sites (similar potential energies) with low activation barrier (activation energy) for hopping between the neighbouring sites.

4. The structure should have preferably a three-dimensional framework, impregnated by open channels for mobile ions to move through.
5. The anion framework should be readily polarizable.

Degree of crystallinity, salt concentration and temperature are the important factors affecting ionic conductivity of polymer electrolytes (*Bruce and Vincent, 1993*). Crystal defects are mandatory for ionic conduction. Declining crystalline phase in the polymer electrolytes triggers the formation of amorphous phase which is the physical state of a polymer where the molecules are in disordered arrangement. These disordered regions create enough voids for ion hopping which leads to increase in ionic conductivity of polymer electrolytes. Ideally, at low salt concentrations, number of charge carriers strongly affects the ionic conductivity. At high salt concentrations, the ionic conductivity is predominantly dependent on the mobility of ions. In polymer electrolytes, long range ion diffusion leads to ionic conductivity which can occur only in the presence of local segmental motions of the polymer host (*Judeinstein et al., 2005; Lonergan et al., 1995*). Number of empirical relations and theories/models are developed/proposed to explain the ion conduction mechanism in different polymer electrolyte systems.

2.2. Ion Transport Mechanism

Earliest known concepts of ion-transport in PEO-salt complexes suggested by *Armand et al. (1979) and Bruce et al. (1993)*, explained that the cations resided inside single/double helices of polyether chains and hopping of these cations through the helices was described as ion-transport mechanism. The anions were thought to occupy nearly immobile positions outside the helix. Later, *Gray (1997)* suggested another model depicting that the ion motion was associated with polymer chain segmental motion due to making and breaking of co-ordination bonds between the polymer and the cations. Gray took into consideration ion-ion and ion-polymer interactions and asserted that ionic motion is either supported by polymer chains or it is the motion from one ionic cluster to another with polymer chains acting as anchor points (*Fig. 2.2*). The mechanism largely depends on salt concentration in polymer electrolytes. Above glass transition temperature, T_g , the ion motion in polymer electrolytes is facilitated by the local motion of the polymer chain segments. This liquid-like motion of polymer segments above T_g causes the surroundings of the polymer matrix to change with time

and strongly affects the charge transport process. Equation of conductivity of a material with different charge carriers is given as (Agrawal and Gupta, 1999),

$$\sigma = \sum_i q_i n_i \mu_i \quad (2.1)$$

where σ is the specific ionic conductivity (the charge transport across a unit cross-sectional area per second per unit electric field applied), n and q are the number of each kind of carrier and its charges respectively and all the variables depend on the material environment. Earlier studies of PEO salt complexes suggested that cations remained inside the single or double helices of polyether chains (Bruce and Vincent, 1993; Gray, 1997), and cation hopping through the helices was thought to be charge transport mechanism. And the nearly immobile anions stood outside these helices.

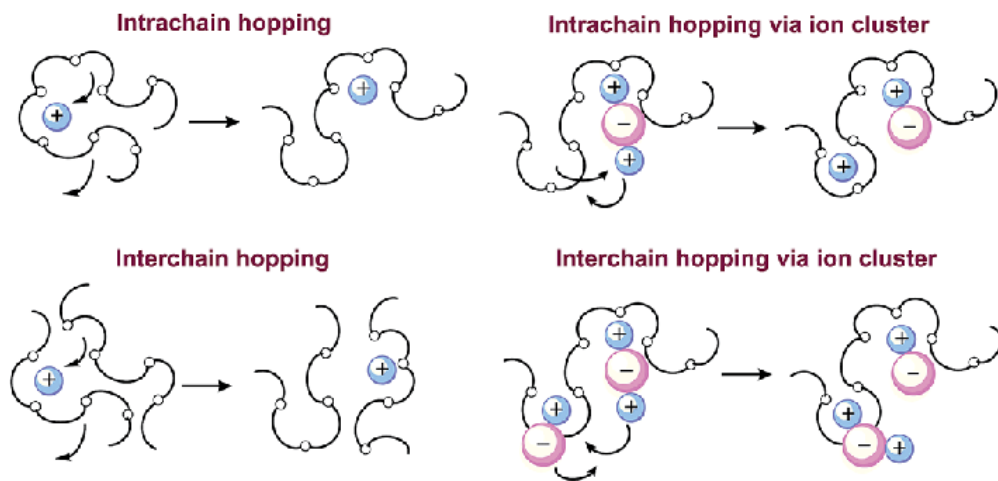


Fig. 2.2 Representation of cation motions in a polymer electrolyte (a) assisted by polymer chain motion only; and (b) taking account of ionic cluster contributions.

<https://www.researchgate.net/publication/280395226>

2.3. Empirical relationship for temperature dependence of conductivity

Theories describing the temperature dependence of conductivity of the polymer electrolyte materials are discussed in this section.

2.3.1. Arrhenius Theory

Swedish scientist, Svante Arrhenius, put forth this theory in 1889 to explain the linear relationship of $\ln \sigma$ vs $1000/T$ plot. Arrhenius behaviour in electrolyte materials is thought to be the consequence of thermal activation of the ions which hop from one vacant site to another by overcoming the energy barrier which exists between the two sites. This energy barrier is the activation energy E_a (Kumar et al., 2006) and the linear relation is given by the equation,

$$\vec{j} = (na^2e^2\nu\vec{E})/kT = \sigma\vec{E} \quad (2.2)$$

where k is the Boltzmann constant, n is the number of defects per unit volume, a is the inter-ionic distance, e is the charge of the ion and σ is the ionic conductivity and ν is the jump frequency or the probability of jumping from one site to another, in absence of any external electric field given as:

$$\nu = \nu_0 \exp(-\Delta G/kT) \quad (2.3)$$

where, ν_0 is the attempt frequency and $\Delta G = \Delta H - T\Delta S$, ΔH and ΔS are the enthalpy and entropy of diffusion respectively. ΔG is the energy of migration and it is the difference between the free energy of ion at the normal lattice point and that atop the barrier. Finally, we reach the form;

$$\sigma = \frac{A}{T} \exp\left(-\frac{E_a}{kT}\right) \quad (2.4)$$

where, $A = ba^2e^2k$ is the pre-exponential factor (b is a proportionality constant) and $E_a = \Delta G + G/2$ is the activation energy for migration and creation of defects. This is the Arrhenius equation (Colomban, 1992; Upadhyay, 2006).

2.3.2. VTF Theory

Typical curvature behaviour of $\ln \sigma$ vs $1000/T$ plot in many polymer electrolyte materials can be explained in terms of Vogel-Tamman-Fulcher (VTF) relationship (Vogel, 1921; Tamman, et al., 1926; Fulcher, 1925). VTF theory explains ion conduction process to be largely dependent on polymer chain segmental motion which provides a free volume into which ion can diffuse under the application of electric field. It is an over simplified relation as it does not take into consideration the ion-ion

interaction and its contribution to conduction mechanism. The VTF relation is given as follows

$$\sigma = AT^{(-1/2)} \left(-\frac{B}{K(T-T_0)} \right) \quad (2.5)$$

where A is pre-exponential factor, $B = E_h + E_j + \frac{\omega}{2\epsilon}$ is the apparent activation energy associated with the hybrid energy which considers the ionic jump E_j , dissociation energy $\frac{\omega}{2\epsilon}$ and energy of hole formation E_h (opposing internal and external pressure to produce a hole responsible for ionic transport), K is the Boltzmann constant, T_0 is the ideal glass transition temperature, typically taken to be 50 K below T_g ([Nava et al., 2016](#); [Lian et al., 2014](#); [Itoh et al., 2013](#)).

2.3.3. WLF Theory

William- Landel- Ferry (WLF) theory is a general extension of VTF relationship. WLF ([Williams et al., 1955](#)) relation explains conduction mechanism in some amorphous materials. WLF relation is as given below

$$\log a_T = \log \left[\frac{R(T)}{R(T_{ref})} \right] = -\frac{C_1(T-T_{ref})}{(C_2+T-T_{ref})} \quad (2.6)$$

Where T_{ref} is a reference temperature, a_T is known as shift factor and C_1 & C_2 are constants. WLF equation affirms that a decrease in T_g could lead to an increase in the ionic conductivity. As it is not explored completely, WLF equation remains under a state of debate and is not generally used to describe transport mechanism in polymer electrolytes.

2.4. Theoretical models of Conductivity

2.4.1 Rouse Model

Rouse model is based on Langevin Dynamics of random networks which is applied to kinetics of polymer electrolytes ([Rouse, 1953](#)). According to this model, ions are assumed to form temporary cross – links between oxygen atoms of polymer backbone which abates structural relaxations. Concentration dependence of conductivity can be determined by applying Nernst – Einstein relation to mean square displacement of ions. After a certain ion concentration, conductivity reaches an optimum and starts

decreasing. Initially, ions have limited motion because they are attached to the polymer host. After some time, the cross-linking of the polymer chains breaks down due to structural relaxations and the ions are free to diffuse through the entire system.

2.4.2 Amorphous Phase Model

Amorphous phase model was designed to explain conductivity enhancement in composite polymer electrolytes ([Wieczorek et al., 1995](#)) composite electrolyte systems are formed by dispersion of inert filler particles such as SiO₂, TiO₂, Al₂O₃ etc in polymer – salt complexes. The amorphous phase model explained increase in conductivity of filler dispersed composite electrolytes as compared to un-dispersed complexes.

2.4.3 Effective Medium Theory

[Nan and Smith \(1991\)](#) proposed this theory to explain electrochemical behaviour of composite systems. Electrical properties of various heterogeneous systems including polymer electrolyte were successfully explained by this model. Influence of inert filler on ionic conductivity could also be well explained by this theory. In such a case, increase in ionic conductivity is associated to a huge defect assembly found on the surface of the filler particles due to formation of space – charge layers. Just like amorphous phase mode effective medium theory considered the presence of three phases in composite polymer electrolytes with each phase having different electrical property.

2.4.4 Free Volume Model

This model was proposed by [Cohen and Turnbull \(1959\)](#) by considering matrix molecules as hard spheres assuming ions to be caged between the *free volume* in between the matrix molecules. If the relaxation of these matrix molecules enlarges this free volume, ion diffusion is facilitated. Statistically, increase in free volume is related to the increase in temperature as,

$$V_f = V_g \{0.025 + \alpha(T - T_g)\} \quad (2.7)$$

where, V_g is critical volume per mole at T_g and T_g is taken to be that temperature at which free volume disappears. α is the coefficient of thermal expansion. T is the experimental temperature (Kumar, 2013). Enhancement of free volume reduces caging of ions leading to an increase in conductivity. VTF/WLF equations represent temperature dependence of conductivity in the vie of free volume model combined with Nernst-Einstein equation.

2.4.5 Configurational Entropy Model (CEM)

Conduction process in case of polymer electrolytes is the consequence of combination of the factors such as, ion-size, polarizability, ion-pairing, ion-concentration and polymer chain length. Free Volume Model did not consider these factors and Adam and Gibbs et al. (1965) gave a modified version of the model. They called it the “Configurational Entropy Model”. According to this model, ion transport mechanism is a co-operative rearrangement of polymer chains instead of inter-site ion hopping. Chain rearrangement probability is given as,

$$W = A \exp \left[\frac{-\Delta\mu S_c^*}{k_B T S_c} \right] \quad (2.8)$$

where, S_c^* is the minimum configurational entropy required for chain rearrangement.

2.4.6 Static Bond Percolation (SBP) Model

Ratner et al. (1987) proposed “Static Bond Percolation Model” which explained ion transport in inflexible network systems at microscopic level. It describes the motion of ion by percolation process i.e. hopping. Hopping rates are portrayed as finite/zero depending upon whether the sites are conjointly available (open) or not (close). Open sites where the mobile charge carriers reside is given as,

$$P_i = \sum (P_j W_{ji} - P_i W_{ij}) \quad (2.9)$$

where, $P_i = P_i(t)$ is the probability of finding the mobile ion species at site i at time t and $W_{ji} = W_{ij}$ is rate of hopping. Links between the localized sites for mobile charge carriers are called “bonds”. In case of polymer electrolytes, the sites are the localized positions and the bonds are the pathways for the mobile charge carriers (Ratner et al., 1987).

In a standard percolation model, the ions jumps which are allowed/not-allowed is given as $W_{ji} = 0$: Probability $1-f = w$: Probability f Static Bond Percolation Model could successfully explain that only the amorphous phase is responsible for ion conduction in polymer electrolytes and the crystalline phase has no conductivity.

2.4.7 Dynamic Bond Percolation (DBP) Model

Dynamic Bond Percolation Model describes systems by considering the dynamic framework rather than rigid network structure model. In this model, the position of open/close bonds is constantly changing. Ion transport is explained as hopping of ions through neighbouring sites (*Ratner et al., 1989; Druger et al., 1983a, 1983b; Druger, 1984*). Above T_g , sites at which the ions can reside, move with respect to one another in the polymer matrix, thus, rearranging the open/close bonds. In this model ion dynamics is controlled by two important relaxation times.

1. Hopping time of charge carrier from one site to the other (hopping life time τ_h)
2. Structural relaxation time of the host polymer (renewal time τ_{ren}).

Then the ion motion is defined as,

$$P_i(t) = \sum (P_j(t)W_{ji} - P_i(t)W_{ij}) \quad (2.10)$$

where, $P_i = P_i(t)$ is the probability of finding the mobile ion species at site i at time t and W_{ij} is the rate of hopping of the charge carrier from site j to site I and the jumps are either permitted or not-permitted as per $W_{ji} = 0$: bond (i, j) not available = w : bond (i, j) available Most of the models discussed above can successfully explain only amorphous and single-phase systems. They cannot give appropriate details of ion – transport mechanism in complex multi –phase systems.

2.5 Frequency dependence of Conductivity

In general, ac and dc measurement techniques are adopted to perform electrical characterization of a material dc measurement method is lucid, but it cannot be used to understand ionic or mixed electronic-ionic systems. Hence ac technique is preferred over dc technique. Number of studies has been carried out to understand frequency dependent behaviour of ionically conducting systems, but we still have a very limited knowledge on this vast subject.

Quite a few theories have been proposed to explain the frequency dependent ac conductivity some of which are briefly discussed below.

2.5.1 Quantum Mechanical Tunnelling (QMT) Model

QMT model explains the rise in conductivity with increase in frequency. **Pollak and Geballe (1961)** first explained tunnelling of electrons in glassy materials based on this model. QMT model explains that the frequency dependence of conductivity arises due to tunnelling of mobile ions between vacant sites through some potential barrier. The expression for conductivity is given as,

$$\sigma(\omega) = \frac{ce^2kT}{\alpha} N^2(E_F) \omega R_\omega^4 \quad (2.11)$$

where, $N(E_F)$ is the density of the states and R_ω is the tunnelling distance at a given frequency ω . And the temperature dependent frequency exponent n , is given as,

$$n = 1 - \frac{4}{\ln\left(\frac{1}{\omega\tau_0}\right)} \quad (2.12)$$

2.5.2 Jump Relaxation Model (JRM)

Jump diffusion of ions in disordered materials was initially explained as arbitrary ion hopping process until Funke and Reiss developed Jump Relaxation Model (*JRM*). According to *JRM*, conductivity dispersion is a close powerful correlation between forward – backward jumps on an ion. Effect of an adjacent ion environment on the potential well of the ion in question and its potential jump relaxation behaviour forms the basis of this model and hence the name *JRM*. Basic assumptions of *JRM* are as follows.

1. All the ions hop in a similar trend.
2. Number of sites is larger than the number of mobile ions.
3. All available sites are equally probable.
4. Repulsive interaction existing between the mobile ions results in “cage effect”.

This concept can be realized pictorially (Fig. 2.3) as suggested by **Funke et al. 1991**. Classical Debye- Huckle theory suggests formation of “*coulomb cage*” due to adjacent ions which modify single particle potential well in such a way that the probability of backward jump increases.

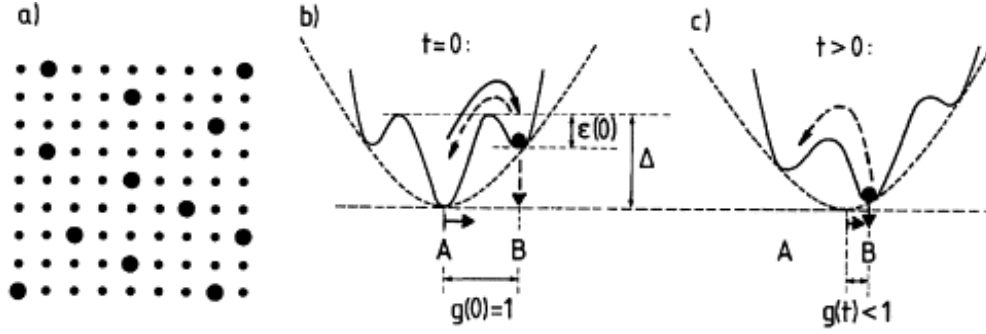


Fig. 2.3 Leitmotif of the jump relaxation model. (a) Ions on a sublattice. (b) Cage-effect potential (broken line) and effective single-particle potential (solid line) after a hop from A to B at time $t = 0$. (c) Development of the potential for $t > 0$. (Funke & Wilmer, 2000).

Equal probability of available sites gets modified due to presence of neighbouring ions. Thus, the possibility of successful ion jump is governed by the relaxation of the coulomb cage at its new location. Probability of backward jump deteriorates velocity auto correlation function due to hops and this causes conductivity dispersion. This negative augmentation is described in terms of $W(t)$. $W(t)$ is the time dependent correlation factor which represents the probability that if an ion makes a forward jump at time $t = 0$ then no backward jump takes place before time t .

$$W(t) = \exp \left\{ -n \left[\frac{\delta(t) - \delta(\infty)}{k_B T} \right] \right\} \quad (2.13)$$

where, $\delta(\infty)$ is the dc activation energy, n is the power law exponent and $\delta(t)$ represents potential barrier at time t . Further the exponent n is given as,

$$n = \frac{\text{initial backward hopping rate}}{\text{initial site relaxation time}} \quad (2.14)$$

This equation implies that if the site relaxation is faster than the backward hop then, $0 < n < 1$ i.e. fractional value n indicates forward hopping and $n \geq 1$ suggests site relaxation to be slower as compared to backward hop.

2.5.3 Dynamic Structural Model (DSM)

Greaves et al., (1985) introduced this model in 1985 to explain classical ion jump to vacant sites and conductivity dispersion in glassy electrolytes. According to this model,

for a multi cation system, motion of charge carriers through the matrix creates vacant sites. The mobile ions play a key part in creation of new sites and in hopping of ions into these sites. Consider the motions of an ion (A^+) from one site to any new site. When (A^+) leaves its original site, it leaves a memory at this site defined as (A^-) say. This site with the memory of previous ion (A^-) acts as “foot-print” for the next ion and hence a conduction pathway is formed. The next A^+ ion will comfortably move to this site. The memory created by outgoing ion (A^+) remains for a certain time (τ), after which the memory is forgotten, and we now call it (C^-). When another (A^+) encounters (C^-), it slows down, and its hopping frequency is defined as follows.

$$W_{(A^+C^-)} = W_{(A^+A^-)} \exp(-k_B T_1/T) \quad (2.15)$$

where, the energy term $k_B T_1$ is defined as mismatch energy i.e. the additional energy required for A^+C^- as compared to A^+A^- . Thus, according to DSM, the target site governs hopping rate of ions.

2.5.4 Small Polaron Tunnelling (SPT) Model

Polaron is a charged particle with local distortion when a strong coupling prevails between the lattice and charge carriers. The charge carrier feels dynamically complacent to be caged/localized at one of the infinite numbers of equivalent sites in the matrix. Polaron/lattice interaction creates distortion in the immediate environment. Such an interaction manifests in the form of a potential well which acts as trapping centre for charge carriers. The term “*small polaron*” is associated with charge carriers which are so localized that their distortion clouds do not overlap. The frequency exponent n described by this model as given by [Emin et al. \(1969\)](#) is,

$$n = 1 - \frac{4}{\ln\left(\frac{1}{\omega\tau_0}\right) - \frac{W_H}{k_B T}} \quad (2.16)$$

Charge conduction mechanism in a variety of different electrolyte systems could be explained successfully using this model ([Dave and Kanchan, 2019](#)).

2.5.5 Correlated Barrier Hopping (CBH) Model

Theoretical knowhow provides two different mechanisms for explaining charge transport, classical hopping and quantum mechanical tunnelling. Neither of the two can explain the temperature dependence of frequency exponent n because in classical

hopping process, n takes a fixed value and in QMT model, hopping length is a function of frequency alone, not considering the barrier height and thermal activation process. Hopping length R_w explains the temperature dependence of n when $n \neq 1$. Hence R_w must be correlated to barrier height in thermally activated process. Then the inter-site length R can be defined by either ‘‘Correlated Barrier Hopping’’ (illustrated in Fig. 2.4) or ‘‘Overlapping Polaron Tunnelling’’. In any case, the inter-site length R and the barrier height W are related as,

$$W = \frac{W_0}{\left(1 - \frac{r_0}{R}\right)} \quad (2.17)$$

where, W_0 is the value of maximum barrier potential. This lowering in the barrier potential from its original value W_0 (ideally considered for a pair of sites at infinite separation) is due to Coulomb interaction between charge carrier and the sites between which the transition is supposed to take place and r_0 is a constant which depends on W_0 and dielectric. Then the frequency exponent n as per Elliot (1987) is given by,

$$n = 1 - \frac{6k_B T}{W_M - k_B T \ln\left(\frac{1}{\omega \tau_0}\right)} \quad (2.18)$$

where, W_M is the maximum barrier height and τ_0 is the characteristic relaxation time. Using first approximation principle, the expression for n can be simplified as,

$$n = 1 - \frac{6k_B T}{W_M} \quad (2.19)$$

This equation shows that n decrease with increase in temperature. Number of studies have successfully employed CBH model to explain the charge transport mechanisms in the polymer systems.

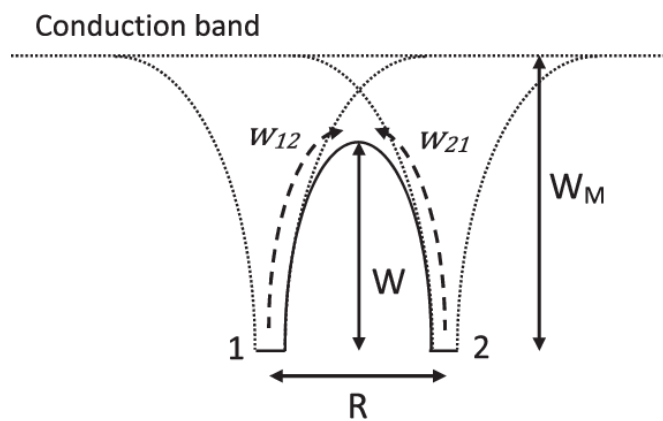


Fig. 2.4 CBH Model: Lowering of barrier height for two closely spaced charge carriers.

https://www.researchgate.net/figure/Pair-model-correlated-barrier-hopping-Trap-levels-1-and-2-separated-by-a-distance-R_fig11_265210796

2.5.6 Asymmetric Double Well Potential (ADWP) Model

Low temperature anomalies of glasses (*Anderson et al., 1972; Philips et al., 1972*) could be explained using the concept of independent two-level tunnelling mechanism (*Pollak et al., 1972*). The term ‘‘Asymmetric Double Well Potential’’ (illustrated in *Fig. 2.5*) was coined by *Gilroy and Philips (1981)*. Classical hopping phenomenon in the systems can be well explained by this model. In this case, two independent states of double well potential are considered which are separated by a barrier V and associated with energy difference Δ .

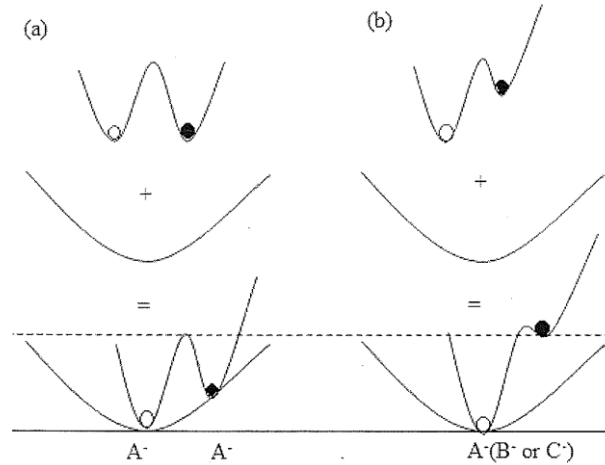


Fig. 2.5 Ion hopping mechanism (at $t=0$, i.e. right after ion has hopped) (a site sensitive model on top and coulomb cage potential below). (*Bunde et al., 1960; Kumar, 2014*).

Considering the two states as two different positions of a charged particle separated by a distance a , the dielectric response of identical ADWP mechanism is given as,

$$\sigma(\omega) = -\frac{Ne^2a^2}{3k_B T} p_1^{eq} p_2^{eq} \frac{i\omega}{1-i\omega\tau} \quad (2.20)$$

$$\tau = \frac{1}{w_1+w_2}$$

And this manifests as a Debye peak with a peak-frequency of $1/\tau$ in the system.

2.6 Conductivity Formulism

Impedance spectroscopy studies impedance of an electrochemical cell over a range of temperatures and frequencies and analyze them in complex impedance plane (*Retter et al., 2010*). Particularly, it is characterized by the measurement and analysis of Z^* (complex impedance) and plotting of this function. In complex plane is known as

Nyquist plots. **Sluyter et al. (1960)** studied the polarization phenomenon of aqueous electrochemical cells using electrochemical impedance spectroscopy and there after it has been widely used as an important tool to analyze electrochemical processes in the field of aqueous electrochemistry (**Badawy et al, 2010; Yuan et al, 2010**). In **1969, Bauerle** for the very first time applied this technique to study basic polarization process in YSZ cell. Ever since, electrochemical impedance spectroscopy has been employed to characterize variety of electrolyte materials including polymers, glasses, polycrystalline composite systems and ionic liquid-based systems. Impedance spectroscopy is an ideal technique to probe electrical properties of solid electrolyte material (**Macdonald, 1992**) in which the frequency independent data gives information about bulk conductivity and total transport phenomenon occurring therein. Impedance frequency data are typically analysed in following three ways.

- (1) Graphical Representation of real part of Z as parametric function of frequency
- (2) Analysing the data for bulk and /or microscopic properties
- (3) Plotting the data in different representations i.e. complex dielectric constant and modules using appropriate mathematical tools.

We use a sine wave in the input for impedance measurements and record the magnitude of response of the system to the electrical stimulus. Applied AC voltage and the resulting current across a cell can be represented as

$$V = V_{max} \sin (wt)$$

$$I = I_{max} \sin (wt + \varphi) \quad (2.21)$$

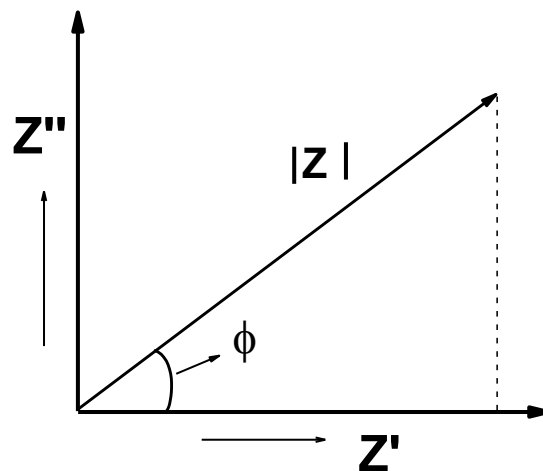


Fig. 2.6 Impedance plot in a complex plane.

where, φ is the phase angle corresponding to the phase difference between the applied voltage and current. Impedance comprises of a frequency independent resistive term R and a capacitive term $1/j\omega C$, $j = \sqrt{-1}$. Magnitude of impedance is given as $|z| = V_{max} / I_{max}$. Relationship between absolute value of $|z|$ and the phase angle φ with real and imaginary parts of impedance (Z' and Z'') is given as

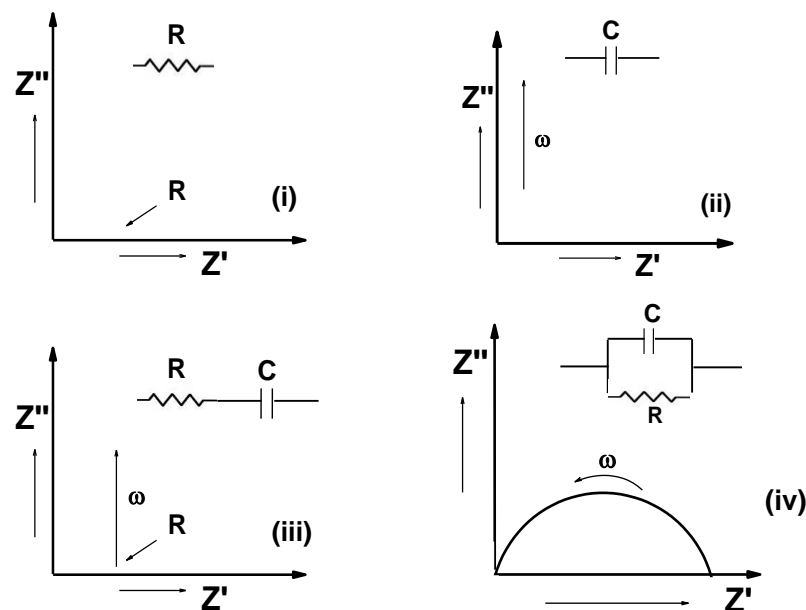
$$\begin{aligned} Z' &= |z| \cos \varphi \\ Z'' &= |z| \sin \varphi \end{aligned} \quad (2.22)$$

Projection of real and imaginary parts of impedance on X- and Y –axis results in a Nyquist diagram which is an implicit function of frequency complex impedance Z^* is given by

$$Z^* = Z' + jZ'' \quad (2.23)$$

2.6.1 Complex Impedance Data Analysis

AC impedance experiments are generally performed over a wide frequency range and the resulting data are interpreted by comparing to equivalent circuits. All sets of impedance data cannot be analysed by single equivalent circuit. There are infinitely many circuits containing minimum number of elements and represent the given set of impedance data extensively. Some of which are illustrated in Figs. 2.7(i-iv) below.



Figs. 2.7(i-iv) Complex Impedance plots for some elementary R , C and RC circuits.

Ionic conductivity is can be perceived as a sequential mechanism which involves successive jumps of an ion over the potential barriers along the electric field direction. This, modelled in a parallel RC circuit is given by,

$$Y^* = Z^* - 1 = R - 1 + j\omega C \text{ or } \frac{1}{Z^*} = \frac{1}{R} + j\omega C \quad (2.24)$$

$$\text{so, } Z^* = \frac{R}{1+j\omega CR} \quad (2.25)$$

and simplifying the above expression by using complex conjugate, we have

$$Z^* = \frac{R(1+j\omega CR)}{1+(\omega CR)^2} \quad (2.26)$$

$$Z' = \frac{R}{1+(\omega CR)^2} \quad (2.27)$$

$$Z'' = \frac{(\omega CR)^2}{1+(\omega CR)^2} \quad (2.28)$$

Between two extreme conditions given as;

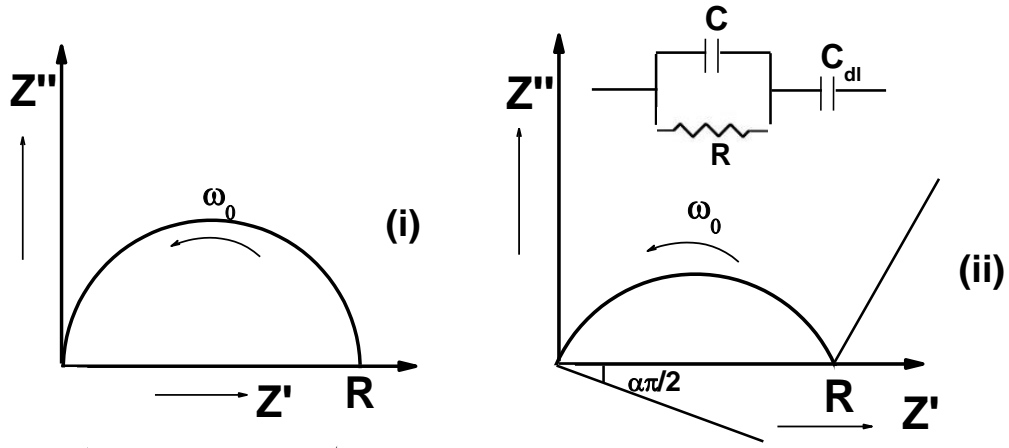
1. $\omega = 0$, $Z' = R$ and $Z'' = 0$ and
2. $\omega = \infty$, $Z' = 0$ and $Z'' = 0$, the values of Z' and Z'' comply as,

$$\frac{R^2}{4} = \left(Z' - \frac{R}{2}\right)^2 + Z''^2 \quad (2.29)$$

This is the equation of a circle with radius $R/2$ and centre at $(R/2,0)$ and is represented in [Fig. 2.7\(iv\)](#). It portrays the response of a resistor R in parallel with capacitor C which will be a perfect semicircle intersecting the real axis at $(R, 0)$.

In Cartesian form, impedance can be written as;

$$Z^*(\omega) = Z[\cos(\varphi) - j \sin(\varphi)] = Z' + jZ'' \quad (2.30)$$



Figs. 2.8(i-ii) Geometric response for an (i) ideal circuit (ii) distributed elements.

The computed data displayed in the complex plane in the form of real and imaginary component as an implicit function of frequency is called the *complex impedance plot*. Some basic complex impedance plots corresponding to R , C and RC circuit network for conductivity measurements in the electrochemical cells, are shown in the **Figs. 2.8(i and ii)**.

There are several other measured or derived quantities related to impedance which often play important roles in Impedance Spectroscopy. The two other quantities complex dielectric constant or dielectric permittivity (ϵ^*) and the modulus function (M^*) are usually defined as (*Jonscher, 1983; Venkatesh and Raghavan, 2005; Macedo et al., 1972; Wubbenhorst and Turnhout, 2002; Cole, 1960*)

$$\epsilon^*(\omega) = \epsilon'(\omega) - i\epsilon''(\omega) = \frac{1}{i\omega C_0 Z^*} \quad (2.31)$$

$$\begin{aligned} M^*(\omega) &= \frac{1}{\epsilon^*(\omega)} = j\omega C_0 Z^* = M'(\omega) + jM''(\omega) \\ &= M_\infty \left[1 - \int_0^\infty \exp(-j\omega t) \left(\frac{d\phi(t)}{dt} \right) dt \right] \quad (2.32) \end{aligned}$$

where, $C_0 = \epsilon_0(A/t)$ is the capacitance of the empty measuring cell of electrode area A and thickness t and ϵ_0 is the dielectric permittivity of free space of value 8.854×10^{-12} F/m.

2.7 Dielectric Properties of Materials

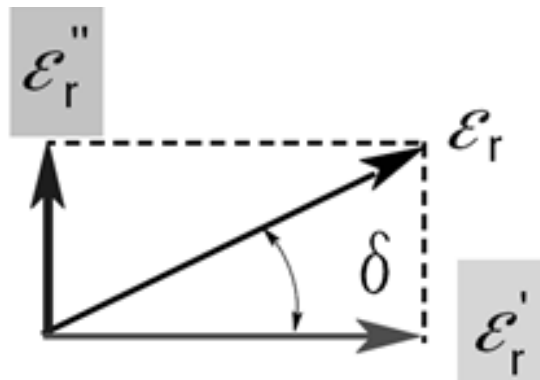
Permittivity and permeability of materials change with change in frequency, temperature, orientation, mixture, pressure and molecular structure of the material. A “dielectric” is defined as a material that could store energy in presence of applied electric field. When a DC voltage is applied across a parallel plate capacitor, it will be able to store more charge in presence of a dielectric material than in absence of it. The charges at the electrode which normally contribute to the electric field are neutralized by the dielectric material and thus the capacity of storage is increased. When an AC voltage is applied across the same capacitor, the resulting current is made up of charging current I_C and a loss current I_l . These losses are represented as a conductance (G) in parallel with a capacitor (C). The complex dielectric constant k consists of a real part k' (representing the storage) and an imaginary part k'' (representing the loss). The following notations can be used interchangeably for the complex dielectric constant interchangeably $k = k^* = \varepsilon^*$

Electromagnetic theory defines electric displacement (electric flux density) D_f as, $D_f = \varepsilon E$ where, $\varepsilon = \varepsilon^* = \varepsilon_0 \varepsilon_r$ the absolute permittivity, ε_r is the relative permittivity, $\varepsilon_0 \approx 8.864 \times 10^{-14} \text{ Fcm}^{-1}$ is the free space permittivity and E is the electric field.

Dielectric permittivity is a complex quantity which describes interaction of a material with an electric field, E ($\varepsilon^* = \varepsilon' - i\varepsilon''$). In the equation, the real part of permittivity (ε') is a measure of how much energy from an external electric field can be stored in the material and the imaginary part of permittivity (ε'') (accounting to the loss factor) is a measure of how dissipative or lossy a material can be to an external electric field. The loss factor ε'' includes both, dielectric and conductivity losses. ε'' is always greater than zero and is usually much smaller than ε' and includes the effects of both dielectric loss and conductivity. Complex permittivity is represented as a simple vector diagram in (Fig. 2.9). The real and imaginary components are 90° out of phase and the vector sum forms an angle δ with the real axis (ε'). The relative “loss” of a material is the ratio of the energy lost to the energy stored. The loss tangent ($\tan \delta$) is defined as the ratio, $\varepsilon''/\varepsilon'$. The dissipation factor is denoted by D and Q is the quality factor.

$$\tan \delta = \frac{\varepsilon''}{\varepsilon'} = D = \frac{1}{Q} = \frac{\text{Energy lost per cycle}}{\text{Energy stored per cycle}} \quad (2.33)$$

For very low loss materials, $\tan \delta \approx \delta$, and the loss tangent can be expressed in angle units, milli-radians or micro-radians.



Figs. 2.9 *Vector diagram for Loss tangent.*

2.7.1 Dielectric Mechanisms

The overall permittivity of a material is a combination of several dielectric mechanisms and polarization effects. Inside a dielectric material, the electric charge carriers are so arranged that they are displaced by external electric field. A dielectric material gets polarized in order to compensate the electric field. Microscopically, several dielectric mechanisms combined contribute to the overall dielectric behaviour of a material.

2.7.1.1 Orientational (Dipolar) Polarization

Atoms combine by sharing one or more of their electrons and form a molecule. In this process of rearrangement, an imbalance in charge distribution occurs leading to a permanent magnetic dipole moment. In absence of external electric field, there is zero net polarization effect due to random orientation of the dipoles. In presence of electric field (E), the torque (τ) acting on the electric dipole will make them rotate and align with the direction of the applied field, thus causing orientational polarization. Complex impedance $Z^*(\omega)$ has both, magnitude (Z) and phase angle φ and can be expressed in polar and Cartesian forms.

2.7.1.2 Electric and Atomic Polarization

When an electric field displaces the nucleus with respect to the surrounding electron, electric polarization occurs. In the presence of an electric field, adjacent negative and positive ions flex and give rise to atomic polarization effect.

2.8 Modulus Formalism

In case of dielectric materials, the unwanted Maxwell-Wagner polarization effects, can be eliminated by considering modulus formalism to represent frequency dependent dielectric or conductivity data. Maxwell-Wagner polarization is the build up of charge between two parallel RC elements in series (*Hodge et al., 1975*). Hence theoretically single loss peak observed in ε'' plots correspond to two peaks of M'' plots. But for Maxwell-Wagner polarization process, the effective resistance of the suspending medium is infinite and hence only single peak is observed in M'' spectra.

The positions and intensities of the peaks correspond to the relaxation phenomenon *Macedo et al (1972)* defined electric modulus as the electric analogy of dynamic mechanical modulus and can be related to complex permittivity as given by **equation (2.31)**. Where, M' and M'' are the real and imaginary parts of the complex modulus M^* . The function $\varphi(t)$ gives the time evolution of the electric field within the material and $\omega = 2\pi f$ is the angular frequency. Analysis of electrical relaxation in terms of complex permittivity $\varepsilon^*(\omega)$, gives relaxational parameters, characteristics of the decay of the displacement vector \vec{D} . The expression for the decay of electric field in time domain can be written as:

$$\vec{E}(t) = \vec{E}(0)\varphi(t) \quad (2.34)$$

where $\vec{E}(0)$ denotes the electric field at time $t = 0$ and $\varphi(t)$ is a macroscopic decay function of the general form

$$\varphi(t) = \int_0^\infty g(\tau_\sigma) \exp\left[-(t/\tau_\sigma)^\beta\right] dt \quad (2.35)$$

where τ_σ is conductivity relaxation time and $g(\tau_\sigma)$ is a normalized density function for relaxation times. Thus, using equations (2.33) and (2.35), we have,

$$M^*(\omega) = M_\infty \int_0^\infty g(\tau_\sigma) \left[\frac{j\omega\tau_\sigma}{1+j\omega\tau_\sigma} \right] d\tau_\sigma \quad (2.36)$$

The decay function $\varphi(t)$ (in equation 2.31) exhibits non exponential behavior in amorphous systems i.e., if there is a distribution of relaxation times. In time domain, the decay function is called stretched exponential introduced by Kohlraush-Williams-Watts (KWW) and is given as:

$$\varphi(t) = \exp \left[- \left(\frac{t}{\tau_\sigma} \right)^\beta \right]; 0 < \beta < 1 \quad (2.37)$$

where τ_σ (conductivity relaxation time) and β (Kohlrausch-Williams-Watts exponent) are the parameters of stretched exponential function. The β parameter has been interpreted either as representatives of a distribution of relaxation times or as characteristic of cooperative motions between charge carriers. The relaxation parameter, which increases with decrease in width of the relaxation time distribution and its values show the degree of deviation from ideal Debye behavior and $\beta \sim 0$ illustrates maximum interaction between ions and the factors affecting the ion transport (*Dave and Kanchan, 2018*).

2.9 Plasticization Theories

Other than ion-transport theories, certain theories have been developed which represent the effect of plasticizers on polymer electrolytes.

Plasticization theories are briefly discussed below.

1. Lubricity Theory

Kilpatrick (1940), Clark (1941), Houwink (1947) developed Lubricity theory which defines plasticizer as a lubricant between the molecules of the polymer. The plasticizer reduces intermolecular friction between the polymer chain molecules by lubricating the motion of the molecules and inhibiting their internal resistance due to sliding. Lubricity theory also assumed polymer macromolecules to have very weak bonds away from their cross – linked sites.

2. Gel Theory

Gel theory is an extension of Lubricity theory and developed by *Aiken and others (1996)*. It states that the plasticizer molecules reduce polymer-polymer interaction by getting in between the chains. The polymers formed by tri-dimensional honeycomb structure have loose polymer molecules along their chains. Hence, a solvation – de-

solvation and aggregation – reaggregation equilibria exists between polymer – plasticizer molecule. Presence of plasticizer in a polymer separates polymer chains from each other making gel-like conduction pathways for ion motion.

Free Volume Theory

The free volume theory of plasticization explained the reduction in polymer glass transition temperature upon addition of plasticizer. The specific volume of polymers decreases linearly with decrease in temperature up to T_g . After this, the specific volume decreases more slowly. The increased specific volume above the glass transition temperature was thought to be due to “free volume” space between molecules. Free volume is typically defined as the difference in specific volume at some temperature and the reference temperature is usually taken to be zero. To determine what volume of plastic would be at absolute zero is theoretically and practically a difficult task, so we consider an approximation. Free volume in polymer is a contribution from various sources such as motion of polymer end groups, motion of polymer side groups and internal polymer motions which are below T_g . After addition of plasticizer in the polymer, the plasticizer molecules like the above-mentioned motions create free volume (*Cadogan et al., 1996; Marcilla et al, 2004*).

2.10. Irradiation

Irradiation has been recurrently used as a powerful tool for probing the ion-polymer interactions. Energetic ions are the basic requirements in such studies. Energetic ions are obtained in various ways such as using radioactive sources like α -particles, fission product emitters or by harnessing nuclear reactions involving neutrons which produce emission of protons, tritons, α -particles or fission products. Other particle ions are obtained by bombarding a suitable target with swift heavy ion (which has been used as source of irradiation in present study). Sporadically arriving cosmic rays are also used for generating high energy particles (*Fink et al., 2005*). For material science applications of swift heavy ion (SHI) beam irradiation, it is mandatory that the no nuclear reactions are taking place inside the sample besides the ones which are induced specially for element connected technique. For this the energy of heavy ions has to be kept below the coulomb barrier to make sure that the impinging ions do not participate in their nuclear reactions (*Mehta, 2000*). Polymer response of irradiation depends upon polymer structure and the characteristics of radiation source used e.g. ion energy and

ion species. When a polymer material interacts with an ion beam, the energetic particle loses energy in two ways, nuclear stopping and electronic stopping. When heavy energy ion beams with energy greater than the Coulomb barrier, hit the target nuclei, they cause atomic displacements or atomic vibrations (phonons). In such case, inelastic collisions (due to nuclear reactions) are not considered. Atomic displacements occur when the colliding particle provides energy greater than the displacement threshold (E_d) to a target atom. Else, the knock-on atoms do not escape their sites and instead their energy dissipates as atomic vibrations. Nuclear stopping is the consequence of momentum transfer from ion to target atom and inter-atomic potential between two atoms. Therefore, nuclear stopping varies with ion-velocity and charges of the two colliding atoms. Electronic stopping is another way in which the energy loss of the incoming heavy ion takes place. Depending on the ion-velocity, orbital electrons of the ion are stripped-off in varying degree. Electronic energy loss is the result of electromagnetic interaction between the positively charged ion and target electrons. It comprises of combination of simultaneous mechanisms namely, glancing collisions (inelastic scattering) with small momentum transfer and knock-on collisions (elastic scattering) with large momentum transfer. In each case, the energy is transferred by electronic excitations and ionization (*Mehta, 2000; Lee, 1999*).

Energetic ions modify the polymer matrix either by getting embedded in to it or by destroying the ordered structure of the material. The SHIs have a large range and hence do not get embedded into the system instead modify the system by disrupting the polymer chains. Both nuclear and electronic stopping are responsible for material modification by SHI. In case of polymer electrolyte materials, irradiation by SHI has led to improved conductivity (*Kumar et al., 2006; Dave and Kanchan, 2019*). The changes in ionic conductivity via SHI irradiation occurs due to two primary processes. One is the chain-scissioning (breaking up of polymer chains) and the other is cross-linking of the polymer chains. Chain-scissioning process leads to disruption of the rigid polymer network structure which increases the amorphosity of the polymer. The ions are then able to move faster in the available free space and lead to an increase in conductivity of the system. In contrast, the process of cross-linking restores the crystallinity of the polymer and hinders the conductivity process. At low ion energy (fluence), atomic displacements occurring as a consequence of nuclear collisions are the primary reason of chain-scissioning in the polymer matrix and hence nuclear

stopping mechanism is useful for explaining the low fluence behaviour of the irradiated electrolyte system. Electronic stopping mechanism becomes important at higher fluence values when the electromagnetic interactions lead to formation of free radicals and chemically active species. Coulomb interactions among these active species cause rigorous bond stretching and segmental motion of the polymer chains which lead to cross-linking and bond-breaking (*Lee, 1999*).

REFERENCES

1. R. W. Cahn, P. Haasen, *Physical Metallurgy*, North-Holland Physics, 1996.
2. P.G. Bruce, C.A. Vincent, *Journal of Chemical Society: Faraday Transactions*, 89 (1993) 3187-2303.
3. P. Judeinstein, D. Reichert, E. R. deAzevedo, T.J. Bonagamba, *Acta Chimica Slovenica*, 52 (2005) 349-360.
4. M. C. Lonergan, A. Nitzan, M. A. Ratner, D. F. Shriver, *The Journal of Chemical Physics*, 103 (1995) 3253- 3261.
5. M. B. Armand, J. M. Chabagno, M. J. Duclot, in *Fast Ion Transport in Solids*, P. Vashishta, J. N. Mundy, G. K. Shenoy (eds.), North-Holland, New York, 1979.
6. F. M. Gray, *Polymer Electrolytes*, The Royal Society of Chemistry, Cambridge Ltd., UK (1997).
7. R. C. Agrawal, R. K. Gupta, *Journal of Material Science*, 34 (1999) 1131-1162.
8. A. Kumar, D. Saikia, F. Singh, D. K. Avasthi, *Solid State Ionics*, 177 (2006) 2575–2579.
9. P. Colomban (ed.), *Proton Conductors: Solids, membranes and gels - materials and devices*, Cambridge University Press, 1992.
10. S. K. Upadhyay, *Chemical Kinetics and reaction dynamics*, Springer 2006.
11. H. Vogel, *Phys. Z.* 22 (1921) 645.
12. G. Tammann, W. Hesse, *Z. Anorg. Allg. Chem.* 156 (1926) 245.
13. G. S. Fulcher, *Journal of American Ceramic Society*, 8 (1925) 339.
14. P. Nava, Guzmán, J. Vazquez-Arenas, J. Cardoso, B. Gomez, I. Gonzalez, *Solid State Ionics*, 290 (2016) 98-107.
15. F. Lian, H.-y. Guan, Y. Wen, X.-r. Pan, *Journal of Membrane Science*, 469 (2014) 67–72.
16. T. Itoh, K. Fujita, K. Inoue, H. Iwama, K. Kondoh, T. Uno, M. Kubo, *Electrochimica Acta*, 112 (2013) 221–229.
17. M. L. Williams, R. F. Landel, J. D. Ferry, *Journal of American Ceramic Society*, 7(1955) 3701.
18. P. E. Rouse, *Journal of Chemical Physics*, 21 (1953) 1272
19. W. Wieczorek, Z. Florjanczyk, J.R. Stevens, *Electrochimica Acta*, 40 (1995) 2251-2258.

20. C. W. Nan, D. M. Smith, *Material Science and Engineering B*, 10 (1991) 99-106.
21. M. H. Cohen, D. Turnbull, *The Journal of Chemical Physics*, 31(1959) 1164-1173.
22. D. Turnbull, M. H. Cohen, *The Journal of Chemical Physics*, 34 (1961) 120-131.
23. G. Adam, J.H. Gibbs, *The Journal of Chemical Physics*, 43 (1965)139-146.
24. M. A. Ratner, In: *Polymer Electrolyte Reviews-1*, J. R. MacCullum and C. A. Vincent (Eds.), Elsevier Applied Science, London, p.173, 1987.
25. M. A. Ratner, A. Nitzan, *Faraday Discussions of the Chemical Society*, 88 (1989) 19-42.
26. S. D. Druger, A. Nitzan, M.A. Ratner, *Solid State Ionics*, (1983a) 1115-1120.
27. S. D. Druger, A. Nitzan, M.A. Ratner, *The Journal of Chemical Physics*, 79 (1983b) 3133-3142.
28. S. D. Druger, *The Journal of Chemical Physics*, 100 (1994) 3979-3984.
29. M. Pollak, T. H. Geballe, *Physics Review*, 122 (1961) 1742-1753.
30. K. Funke, *Radiation Effects and Defects in Solids*, 119-121 (1991) 463-468.
31. G. N. Greaves, *Journal of Non-crystalline Solids*, 71 (1985) 213-217.
32. D. Emin, T. Holstein, *Annual Physics*, 53 (1989) 439-520.
33. G. Dave, D. K. Kanchan, *Radiation Physics and Chemistry*, 161 (2019) 87-94.
34. S. R. Elliot, *Advances in Physics*, 36:2 (1987) 135-217.
35. P. W. Anderson, B. I. Halperin, C. Varma, *Philosophical Magazine*, 25 (1972) 1-9.
36. W. A. Philips, *Journal of Low Temperature Physics*, 7 (1972) 351-360
37. M. Pollak, G. E. Pike, *Physics Review Letters*, 28 (1972) 1449-1451
38. K. S. Gilroy, W. A. Philips, *Philosophical Magazine B*, 43 (1981) 735-746.
39. U. Retter, H. Lohse *Chapter II.5, Electrochemical Impedance Spectroscopy*, F. Scholz (ed.), *Electroanalytical Methods*, 2nd ed., Springer-Verlag Berlin Heidelberg 2010.
40. J. H. Sluyters, *Rec. Trav. Chim.* 79 (1960) 1092-1100.
41. W.A. Badawy, N.H. Hilal, M.El-Rabiee, H. Nady, *Electrochimica Acta*, 55 (2010) 1880-1887.
42. X. Z. Yuan, C. Song, H. Wang, J. Zhang, *Electrochemical Impedance Spectroscopy in PEM Fuel Cells*, Springer-Verlag London Ltd. 2010.
43. J. E. Bauerle, *Journal of Physics and Chemistry of Solids*, 30 (1969) 2657.
44. J. R. Macdonald, *Journal of Electroanalytical Chemistry*, 223 (1987) 25-50.

45. A. K. Jonscher, *Dielectric relaxation in Solids*, Chelsea Dielectric Press, London, 1983.
46. M. S. Venkatesh, G. S. V. Raghavan, *Canadian Biosystems Engineering*, 47 (2005) 7.15-7.30.
47. P. B. Macedo, C.T. Moynihan, R. Bose, *Physics and Chemistry of Glasses*, 13(1972) 171-179.
48. M. Wubbenhorst, J. V. Turnhout, *Journal of Non-crystalline Solids*, 305 (2002) 40-49.
49. R. H. Cole, *Annual Review. Physical Chemistry*, 11(1960) 149-168.
50. I. M. Hodge, M. D. Ingram, A. R. West, *Journal of Electroanalytical Chemistry*, 58 (1975) 429.
51. G. Dave, D. K. Kanchan, *Indian Journal of Pure and Applied Physics*, 56 (2018) 978-988.
52. A. J. Kilpatrick, *Journal of Applied Physics*, 11 (1940) 255.
53. F. W. Clark, *Chem. Ind.* 60(1941) 225.
54. R. Houwink, *Proc. XI Cong. Pure Appl. Chem.*, London, 1947, p. 575–583.
55. W. Aiken, T. Alfrey, A. Janssen, H. Mark, *Journal of Polymer Science*, 2 (1947) 178-198.
56. D. F. Cadogan, C. J. Howick, *Plasticizers in Kirk-Othmer Encyclopedia of Chemical Technology*, John Wiley and Sons, New York (1996).
57. A. Marcilla, M. Beltran, *Mechanisms of Plasticizer Action in Handbook of Plasticizers*, G. Wypych, (ed.), Chem. Tec. Publishing, Toronto, (2004) 107–120.
58. D. Fink, L. T. Chadderton, *Brazilian Journal of Physics*, 35 (2005) 735-740.
59. G. K. Mehta, *PINSA*, 66 (2000) 653-674.
60. A. Kumar, D. Saikia, F. Singh, D. K. Avasthi, *Solid State Ionics*, 177 (2006) 2575-2579.
61. E. H. Lee, *Nuclear Instruments and methods in Physics Research B*, 151 (1999) 29-41.